Table II shows a comparison of the reduction rates of several metalloporphyrins and reconstituted metallomyoglobins by dithionite, all of which go by way of SO_2^-. The Fe^{III}–Mb/$S_2O_4^{2-}$ reaction gives a two-term rate law,[4] where SO_2^- reduces H_2O–Mb (pK_{a1} = 8.9) several hundred times faster than HO–Mb. The same trend is noted with aquo/hydroxo iron(III) protoporphyrin[9] and aquo/hydroxo cobalt(III) tetrakis(*N*-methyl-4-pyridiniumyl)-porphyrin (TMPyP).[13] For manganese(III) hematoporphyrin,[8] k_{H_2O}/k_{OH} = 3, and with Fe–CyDTA^{2-} and Fe^{III}–Mb, the ratio[44] is ca. 6. All are consistent with outer-sphere electron transfer and stabilization of the oxidized state by the negative hydroxide.[4,45,46] Co^{III}–Mb (and also low-spin d^6 Ru^{II}–Mb[20] and Rh^{III}–Mb[47]) presumably has both distal and proximal imidazoles coordinated to the metal, and the dithionite reduction kinetics[3] indicated that two such forms (rotational isomers?) were present in the haloprotein. The rate law suggests predissociation of one ligand from Co(III) before reduction of SO_2^-. The Ru^{II}–Mb/CO reaction[30] is also biphasic and dissociative.

At pH 7 with 2.5 mM $S_2O_4^{2-}$, the half-lives for reduction of metallomyoglobins are 9 × 10^{-2} s for Fe^{III}–Mb,[4] 11 s for Mn^{III}–Mb, and 1.4 and 19 min, respectively, for the two forms[3] of Co^{III}–Mb. For metallomesoporphyrins in pyridine/water, the SO_2^- reduction rates[12] are also in the order Fe > Mn > Co in the ratio 10^4:10^2:1.

Fe^{II}–EDTA at pH 6.8 will reduce Fe^{III}–Mb ($Fe^{III/II}$–Mb, $E°$ = 0.05 V at pH 7), and under similar conditions we find no reduction of Mn^{III}–Mb. This is consistent with the fact that iron(III) porphyrins ($Fe^{III/II}$–TMPyP, $E°$ = +0.18 V vs. NHE[48]) have reduction potentials 150–180 mV more positive that the corresponding manganese(III) porphyrin ($Mn^{III/II}$–TMPyP, $E°$ = –0.01 V[49]). Mn^{III}–Hb is 122 mV more stable than Fe^{III}–Hb[50] at pH 7. The self-exchange rate constant (k_{11}) for high-spin $Fe^{III/II}$–TMPyP[51] is 1.2 × 10^6 M^{-1} s^{-1}, and 7.5 × 10^5 M^{-1} s^{-1} has been estimated for $Fe^{III/II}$–Proto from the Fe^{III}–Proto/$S_2O_4^{2-}$ reaction.[52] The average k_{11} for several manganese(III/II) porphyrins[26] is 2.9 × 10^3 M^{-1} s^{-1}, where the Fe–TMPyP and Mn–porphyrin results are both based on $Ru(NH_3)_6^{2+}$ reductions. With use of the relative Marcus theory[53] and with the same k_{11}'s assumed for the metalloproteins and metalloporphyrins, the ratio Fe^{III}–Mb/Mn^{III}–Mb for SO_2^- reductions is in the range 10^2–10^3 for differences in potential (ΔE) of 0.1 and 0.2 V. This is in good agreement with the observed (Table II) ratio of 385. From the Fe^{III}–Mb/Fe–EDTA^{2-} reaction,[54] k_{11}^{cor} for $Fe^{III/II}$–Mb = 1.3 × 10^{-1} M^{-1} s^{-1} (3.9 × 10^{-2} for Fe–CyDTA^{2-} as the reductant), which is substantially lower than ca. 10^6 M^{-1} s^{-1} for the iron porphyrins themselves. While the rate ratio agreement may be fortuitous, an implication may be that the iron and manganese porphyrin k_{11}'s are lowered to the same relative extent in their metalloglobin forms. Further experiments on this theme are in progress.

Acknowledgment. This work was supported in part by Howard University NIH Biomedical Research Grant 5-SO-6-RR-08016-9 and PHS Grant GM-07700-05 and at the NBS by the Office of Basic Energy Sciences, Department of Energy.

Registry No. $S_2O_4^{2-}$, 14844-07-6; histidine, 71-00-1.

(44) Cassatt, J. C.; Marini, C. P.; Bender, J. W. *Biochemistry* **1975**, *14*, 5470–5475.
(45) Reid, J.; Hambright, P. *Inorg. Chem.* **1978**, *17*, 2329–2330.
(46) Ridsdale, S.; Cassatt, J. C.; Steinhardt, J. *J. Biol. Chem.* **1973**, *248*, 771–776.
(47) Aoyama, Y.; Aoyagi, K.; Toi, H.; Ogoshi, H. *Inorg. Chem.* **1983**, *22*, 3046–3050.
(48) Forshey, P. A.; Kuwana, T. *inorg. Chem.* **1981**, *20*, 693–700.
(49) (a) Harriman, A. *J. Chem. Soc., Dalton Trans.* **1984**, 141–146. (b) Langley, R.; Hambright, P. *Inorg. Chem.* **1985**, *24*, 1267–1269.
(50) Bull, C.; Fischer, R.; Hoffman, B. R. *Biochem. Biophys. Res. Commun.* **1974**, *59*, 140–144.
(51) Pasternack, R. F.; Spiro, E. G. *J. Am. Chem. Soc.* **1978**, *100*, 968–972.
(52) Dixon, D. W.; Barbush, M.; Shirazi, A. *Inorg. Chem.* **1985**, *24*, 1081–1087.
(53) k_{Fe-Mb}/k_{Mn-Mb} = $[(k_{11}(Fe)/k_{11}(Mn))(10\ \exp(16.9\Delta E))]^{1/2}$. See: Marcus, R. *Annu. Rev. Phys. Chem.* **1964**, *15*, 1964–1985.
(54) Mauk, G. A.; Gray, H. B. *Biochem. Biophys. Res. Commun.* **1978**, *86*, 206–210.

Contribution from Ames Laboratory—DOE[1] and the Department of Chemistry, Iowa State University, Ames, Iowa 50011

NMR Study of Carbon-13 in Two Zirconium Iodide Cluster Carbides, $CsZr_6I_{14}C$ and $Zr_6I_{12}C$

C. G. Fry, J. D. Smith,[2] B. C. Gerstein,* and J. D. Corbett*

Received March 4, 1985

The inclusion of light nonmetals, carbon especially, in the center of a variety of octahedral M_6X_{12}-type clusters (M = Zr, rare-earth metal; X = Cl, Br, I) has been recently reported.[3-9] The positions of the heavy atoms in the structures of these phases have been well established by single-crystal X-ray diffraction studies. However, the location—indeed the identity and even the presence—of the light nonmetal within the cluster may be more ambiguous in an X-ray study, especially in a compound where the scattering is dominated by the heavier halides and/or secondary extinction effects obscure the presence of the interstitial atom.[9] One example where both of these factors were involved is the misconception of $Zr_6I_{12}C$ as "Zr_6I_{12}".[10,11]

The two phases studied here both contain nominally octahedral clusters of Zr_6I_{12}, the Zr_6I_{14} stoichiometry arising from additional iodine atoms that bridge between the clusters. The X-ray diffraction results show a slightly compressed trigonal-antiprismatic Zr_6 unit (D_{3d} symmetry) in $Zr_6I_{12}C$ (d(Zr–Zr) = 3.35 and 3.28 Å) while in $CsZr_6I_{14}C$ the mode of intercluster bridging produces a tetragonal compression of the cluster but with metal–metal distances of about the same magnitude (3.32 and 3.26 Å), the required C_{2h} symmetry of the metal cluster in fact being rather close to D_{2h}. According to diffraction studies, the carbon (or other) interstitial atom is at the inversion center within each cluster with refined values for d(Zr–C) of 2.259 (1) Å in $Zr_6I_{12}C$ and 2.349 (1) plus 2.265 (1) Å in $CsZr_6I_{14}$. The cesium compound is properly paramagnetic but apparently with an orbital degeneracy such that electron spin–lattice relaxation prevents observation of an EPR signal between 4 and 300 K at 0–13 kG.[9]

To provide information complementary to the X-ray diffraction results, nuclear magnetic resonance spectra of ^{13}C in powdered $CsZr_6I_{14}{}^{13}C$ and $Zr_6I_{12}{}^{13}C$ have been measured. Well-crystallized samples of about 0.4 and 0.2 g, respectively, were prepared as before[9] in virtually quantitative yields from the reaction (850 °C, 2 weeks) of zirconium metal, ZrI_4, CsI (for $CsZr_6I_{14}C$), and 99% enriched ^{13}C graphite in welded Ta tubes that were in turn jacketed in fused silica containers. Both samples were single phase by Guinier powder diffraction, i.e., ≥~97% pure.

The ^{13}C spectra were all taken at 55.35 MHz on a home-built spectrometer similar to that described previously.[12] Typically, 32500 accumulations were taken of the free-induction decay (FID) under a single pulse excitation, with appropriate phase cycling (alternate pulses 180° out of phase) to minimize dc offset. The recycle time between scans was 0.2 s. The 90° preparation pulses were 8 μs long.

(1) Operated for the U.S. Department of Energy by Iowa State University under Contract No. W-7405-Eng-82. This research was supported by the Office of Basic Energy Sciences, Chemical and Materials Sciences Divisions.
(2) Present address: Photosystems and Electronic Products Dept., Du Pont Experimental Station, Wilmington, DE 19898.
(3) Warkentin, E.; Masse, R.; Simon, A. *Z. Anorg. Allg. Chem.* **1982**, *491*, 323.
(4) Warkentin, E.; Simon, A. *Rev. Chem. Miner.* **1983**, *20*, 488.
(5) Ford, J. E.; Corbett, J. D.; Hwu, S.-J. *Inorg. Chem.* **1983**, *22*, 2789.
(6) Hwu, S.-J.; Corbett, J. D.; Poeppelmeier, K. R. *J. Solid State Chem.* **1984**, *57*, 43.
(7) Smith, J. D.; Corbett, J. D. *J. Am. Chem. Soc.* **1984**, *106*, 4618.
(8) Ziebarth, R. P.; Corbett, J. D. *J. Am. Chem. Soc.* **1985**, *107*, 4571.
(9) Smith, J. D.; Corbett, J. D. *J. Am. Chem. Soc.* **1985**, *107*, 5704.
(10) Corbett, J. D.; Daake, R. L.; Poeppelmeier, K. R.; Guthrie, D. H. *J. Am. Chem. Soc.* **1978**, *100*, 652.
(11) Guthrie, D. H.; Corbett, J. D. *Inorg. Chem.* **1982**, *21*, 3290.
(12) Gerstein, B. C.; Chow, C.; Pembleton, R. G.; Wilson, R. C. *J. Phys. Chem.* **1977**, *81*, 565.

0020-1669/86/1325-0117$01.50/0

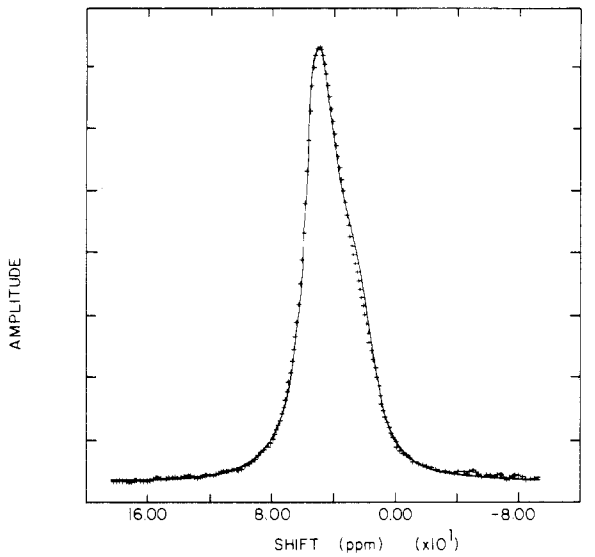

Figure 1. Solid-state NMR spectrum of ^{13}C in $CsZr_6I_{14}C$ as a function of increasing shielding (Me_4Si at 0 ppm). Crosses are experimental points; the smooth line is a least-squares fit with axially symmetric shielding.

The Fourier transform of the FID of ^{13}C in $CsZr_6I_{14}C$ is shown in Figure 1. The shift scale has that for Me_4Si as the origin, and positive shifts are deshielded (downfield). Also shown is the fit of the theoretical expression to the NMR spectrum of the powdered sample that is achieved with a least-squares routine[13] assuming axially symmetric shielding. The main features of the $CsZr_6I_{14}C$ spectra are as follows:

(a) There is only one ^{13}C shielding tensor, as expected. Since the ^{13}C is buried in the cluster, differences in bonding between clusters in different structures might be expected not to affect the ^{13}C electronic environment.

(b) The shielding is axially symmetric, in confirmation of the X-ray structure that shows a nearly square-bipyramidal zirconium environment about the carbon.

(c) $\sigma_\parallel$ (15 ppm) is shielded (upfield) from $\sigma_\perp$ (54 ppm), in agreement with the shorter Zr–C bonds along the approximate C_4 axis of the cluster. (One must still be cautious about interpreting chemical shifts in such a way; see ref 14.)

(d) The carbon is shielded relative to most carbon tensors in organic compounds, and in fact the isotropic value and anisotropy are very similar to those of carbon in a primary methyl group. The relatively small value of the anisotropy suggests that the bonding overlap is fairly symmetric and that perhaps the main difference between $\sigma_\parallel$ and $\sigma_\perp$ originates from the difference in bond lengths. The latter difference has been shown to depend in turn on the asymmetry of the bonding of the terminal iodine atoms at each zirconium vertex.[9]

(e) The spin–lattice relaxation time of carbon in the paramagnetic[9] $CsZr_6I_{14}C$ was determined with use of an inversion-recovery experiment. The value of T_1 was found to be 4 ± 3 ms. This result is not in disagreement with that expected for carbon coupled to the quadrupolar zirconium and iodine nuclei. The electron spins close to the carbon must have spin–lattice transition rates so large that the electron spin is decoupled from the carbon nucleus.

Surprisingly, an accurate measurement of the shielding of ^{13}C in the structurally similar $Zr_6I_{12}C$ has not been obtained, mainly because of the extreme broadness of the signal. But it is clear that the pattern for a single-phase sample of $Zr_6I_{12}C$ runs from at least 28 to 480 ppm, with an isotropic value of 250–300 ppm. The value of 480 ppm is the greatest deshielding ever reported for ^{13}C. Spin counting has confirmed that all the ^{13}C is being observed, and it appears that the signal is again more intense downfield than upfield (axial symmetry cannot be assigned yet).

For comparison, metal carbonyls exhibit isotropic shifts to 360 ppm, with a range of shifts >400 ppm,[15] and inorganic carbides show shift values[16] between +350 and −100 ppm, the largest anisotropy being in boron carbide, where the isotropic shift is about 300 ppm. A plausible source of the relative deshielding in $Zr_6I_{12}C$ is a substantial paramagnetic term in the chemical shift, an effect that is often seen in magnetic susceptibility measurements on such materials. However, the contrasting behavior of $CsZr_6I_{14}C$ vs. $Zr_6I_{12}C$ is not understood. No drastic differences in the carbide cluster bonding are indicated by the results of extended Hückel calculations[9] on isolated $Zr_6I_{18}C^{n-}$ ($n = 5, 6$) clusters, that is, on Zr_6I_{12} units plus six terminal iodides with cluster geometries as found in $CsZr_6I_{14}C$ and $Zr_6I_{12}C$.

Registry No. $CsZr_6I_{14}C$, 98193-80-7; $Zr_6I_{12}C$, 98169-75-6.

(13) Murphy, P. DuBois; Gerstein, B. C. "Analysis and Computerized Fitting of the Lineshape of the NMR Powder Pattern", Report No. IS-4516; Ames Laboratory: Ames, IA 50011.
(14) Mehring, M. "Principles of High Resolution NMR in Solids", 2nd ed.; Springer-Verlag: New York, 1983; Chapter 7.
(15) Gleeson, W.; Vaughan, R. W. *J. Chem. Phys.* **1983**, *78* (9), 5384.
(16) Duncan, M. *J. Am. Chem. Soc.* **1984**, *106*, 2270.

Contribution No. 7178 from the Arthur Amos Noyes Laboratory of Chemical Physics, California Institute of Technology, Pasadena, California 91125, and Contribution from the Departments of Chemistry, University of Oklahoma, Norman, Oklahoma 73019, and University of Cincinnati, Cincinnati, Ohio 45221

Crystal Structure of $[Co(CoL_3)_2]_2(SO_4)Cl_4$: Corrigendum

Richard E. Marsh,[1] Mary Jane Heeg,[2] and Edward Deutsch*[3]

Received April 17, 1985

The crystal structure of $(Co(Co(SCH_2CH_2NH_2)_3)_2)_2(SO_4)Cl_4$, reported[4] in space group $P\bar{1}$ with cell constants $a = 11.803$ (3) Å, $b = 17.227$ (8) Å, $c = 17.239$ (4) Å, $\alpha = 83.24$ (2)°, $\beta = 69.98$ (2)°, and $\gamma = 69.99$ (3)°, has been recast and refined in a more appropriate space group. The matrix

$$\begin{matrix} 0 & 1 & -1 \\ -1 & 1 & 1 \\ 1 & 0 & 0 \end{matrix}$$

transforms the triclinic axes to the tetragonal axes $a = 22.892$ Å, $b = 22.907$ Å, and $c = 11.803$ Å, and the transformed coordinates are consistent with the space group $I4_1/a$ (No. 88, origin at $\bar{1}$) with $a = b = 22.900$ Å. The transformed reflection set generated 2724 independent reflections of which 2210 were observed ($I_o \geq 3\sigma(I)$); the R value for averaging equivalent reflections was 0.031. The new symmetry requires $^1/_2$ cation per asymmetric unit and $Z = 4$ for the title formula. The central cobalt atom (Co2) occupies a crystallographic inversion center; the sulfato sulfur atom (S13) and one of the chloride anions (Cl1) occupy sites of $\bar{4}$ symmetry. All other atoms are in general positions. Refined atomic coordinates, thermal parameters, assumed hydrogen parameters, and structure factors have been deposited as supplementary material.

The tetragonal description refines to the same R values as does the triclinic description and yields no significantly different bond lengths or angles.

Supplementary Material Available: Listings of atomic positional parameters, thermal parameters, hydrogen positional parameters, and observed and calculated structure factors (15 pages). Ordering information is given on any current masthead page.

(1) California Institute of Technology.
(2) University of Oklahoma.
(3) University of Cincinnati.
(4) Heeg, M. J.; Blinn, E. L.; Deutsch, E. *Inorg. Chem.* **1985**, *24*, 1118–1120.

0020-1669/86/1325-0118$01.50/0